



Pergamon

Acta Materialia 50 (2002) 1275–1287



www.actamat-journals.com

Antiphase boundaries in GaP layers grown on (001) Si by chemical beam epitaxy

V. Narayanan^{1a}, S. Mahajan^{a,*}, K.J. Bachmann^b, V. Woods^c, N. Dietz^c

^a Department of Chemical and Materials Engineering and Center for Solid State Electronics Research, Arizona State University, Tempe, AZ 85287-6006, USA

^b Department of Materials Science and Engineering, North Carolina State University, Raleigh, NC 27695-7919, USA

^c Department of Physics, North Carolina State University, Raleigh, NC 27695-7919, USA

Received 5 October 2001; accepted 22 October 2001

Abstract

We have investigated the origin of contrast features observed in coalesced GaP islands, deposited by chemical beam epitaxy on (001) Si, by high resolution transmission electron microscopy and conventional dark field electron microscopy. Our results indicate that these features are antiphase boundaries (APBs) lying on {110} planes. Image simulations have been performed to show that APBs can only be seen under specific defocus conditions in high resolution lattice images. The observed contrast is attributed to the presence of Ga–Ga and P–P wrong bonds at APBs. A model is proposed to show that the coalescence of GaP islands on the same Si terrace may not produce APBs, and the formation of such boundaries may require the presence of monoatomic steps, separating the coalescing islands. © 2002 Published by Elsevier Science Ltd on behalf of Acta Materialia Inc.

Keywords: Transmission electron microscopy (TEM); Epitaxy; GaP; Islands; Antiphase domains

1. Introduction

Antiphase boundaries (APBs) in III–V zinc-blende semiconductors can form during growth across monoatomic steps on (001) Si [1,2]. The occupation of the fcc sublattices is exchanged across the boundary, such that the crystal structure is identical on either side of the boundary and no

unsatisfied bonds exist at the APB. However, the wrong III–III and V–V bonds would be present at the APB. Strain accommodation at these wrong bonds results in relaxation of atoms at the APB boundary away from the perfect crystal positions [3,4]. In addition, such defects are expected to be electrically active and are a concern in device operation [5].

To prevent the formation of such antiphase domains, a step-doubling mechanism has been suggested involving tilting of the Si substrate around one of the two <110> directions lying in the (001) planes [1,6]. Such a tilt results in two different types of steps which differ only in the orientation of dangling bonds with respect to the step edge.

* Corresponding author. Tel.: +1-602-9659710; fax: +1-602-9650037.

E-mail addresses: vrjayna@us.ibm.com (V. Narayanan); smahajan@asu.edu (S. Mahajan).

¹ Present address: IBM T.J. Watson Research Center, Yorktown Heights, NY 10598, USA.

Aspnes and Ihm [6] have shown that a *type A double step* (in their terminology a step with dangling bonds parallel to the step edge) is energetically the most favorable configuration. To produce double steps, high temperature annealing of the vicinal silicon surface is required. However, APB-free growth may be achieved in the absence of double steps. The growth of single domain GaAs (for example) has been explained in terms of APB annihilation [7,8] or selective nucleation of GaAs on one kind of Si (001) steps [9]. Thus, the physical insights into origins of APBs in the growth of III–V semiconductors on Si are still lacking.

Tafto and Spence [10] have used a convergent beam electron diffraction (CBED) technique to identify APBs in the zinc-blende structure. This technique is widely used to identify APBs within epitaxial layers of GaAs/Si [11,12], GaAs/Ge [13] and GaP/Si [14]. Using this method, the direction of crystal polarity can be identified by observing asymmetries in dynamical diffraction contrast of reflections from crystal planes of opposite polarity. Such contrast arises when the Ewald sphere intercepts for example a weak {002} reflection plus two or more higher order, odd indexed reflections. Depending on the type of cation and anion, high order reflections interfere constructively or destructively with direct scattering into the {002} reflections. The interference manifests itself in CBED discs as a bright cross or a dark cross for constructive and destructive interference, respectively. The (002) reflection on one side of an edge on APB would change to the (00 $\bar{2}$) on the other side since all $hkl = > \bar{h}\bar{k}\bar{l}$. When one obtains a dark cross in the (002) disc, then across the APB the disc should have a bright cross. Specific features of the structure factor for the zinc-blende structure also lead to changed diffraction contrast across an APB using certain superlattice reflections. This kind of contrast can also be used to identify such boundaries. Holt [15] showed that the (200) type reflection produces a phase change of π across the APB and would exhibit strong APB contrast during conventional dark-field (CDF) imaging. CDF imaging using the {200} reflection should reveal strong APB contrast and identification of APBs by this procedure has been demonstrated [14,16,17].

In this paper, we have investigated the origin of APBs in coalesced GaP islands grown on (001) Si substrates by high resolution transmission electron microscopy (HRTEM) and CDF. The emphasis is to discern APBs within thin films <60 nm by TEM.

2. Experimental details

The GaP films were grown on exactly oriented (001) Si for by pulsed chemical beam epitaxy (PCBE). The (001) Si wafers were cleaned using a standard RCA clean. During growth the heated Si substrate was exposed to pulses of tertiarybutylphosphine (TBP) and triethylgallium (TEG) under a steady activated hydrogen background pressure [18]. Using a cycle time of 5 s, TEG flow of 0.05 sccm was pulsed into the reactor for 300 ms per cycle under continuous TBP and hydrogen flow of 0.6 and 5.0 sccm, respectively. The overall pressure during deposition was between 10^{-4} and 10^{-5} Torr. The GaP epilayer for this APB experiment was grown for 500 s at 420 °C.

Samples for transmission electron microscopy (TEM) were prepared using the standard ‘sandwich’ technique followed by dimpling and ion milling until electron transparency. Structural analysis of the epitaxial layers was performed in cross-section by CDF and HRTEM. This study was carried out on a JEM-4000EX microscope operating at 400 kV that has an interpretable resolution of 0.16 nm. Localized spatial information from HRTEM micrographs was obtained by digital diffractograms (DDFs). The method is based on measurements of interplanar spacings in reciprocal space and can be used to determine the frequency and amplitude of lattice images. Since each fringe in a high-resolution lattice image corresponds to a characteristic spot in the amplitude of the of the Fourier transform (diffractogram) of a selected image region, lattice-fringe spacings and angles can be measured from spot positions with respect to the center of the diffractogram.

Image simulation was performed using the *Cerius* [19] simulation program. The *HRTEM* module within this program simulates dynamical electron diffraction patterns and real space images

by the multislice technique. In our simulation, we have created an APB by taking two identical GaP crystals, translating one of the crystals by $\frac{a}{4}[111]$, thereby simulating a monatomic step on Si, and then joining the two crystals (using the *Interface* module). In making this interface, the common direction for the left and right side of the crystal was aligned along the $[1\bar{1}0]$ direction with the common plane being (110). When viewing along the $[1\bar{1}0]$ direction, the thickness of the crystal parallel to the $[001]$ and $[110]$ directions was maintained at 2 nm for each direction. The thickness of each successive slice was 0.4 nm. The incident beam was propagated along the $[1\bar{1}0]$ direction through 50 such crystal slices to a thickness of 20 nm. The microscope parameters used were those specified for the JEM 4000EX at Arizona State University. This consisted of an acceleration voltage of 400 kV, spherical aberration coefficient (C_s) of 1 mm, a defocus spread of 8 nm and a beam spread of 0.8 mrad. The final simulation was a through thickness, through focal series and exhibited the change in image contrast due to these parameters.

3. Results

Fig. 1 is a CDF cross-sectional TEM micrograph, obtained using the (002) superlattice reflection, of a GaP epilayer grown on (001) Si for 500s



Fig. 1. A DF-TEM micrograph obtained using the (002) reflection, of a GaP epilayer on (001) Si after 500s of growth at 420 °C. Notice the contrast change across boundaries indicated by arrows.

at 420 °C. This micrograph shows two-dimensional defects denoted by arrows across which the image contrast changes. Intersecting and non-intersecting $\{111\}$ twins are also visible. Fig. 2 is an HRTEM $[1\bar{1}0]$ cross-sectional image of a (001) GaP epitaxial layer deposited at 420 °C after 500 s of growth. The columnar defect A denoted by arrows intersects a microtwin T and extends from the epilayer surface to the GaP/Si interface. The insert in Fig. 2 is a magnified image of the intersection of defect A with a twin. This figure indicates that a slight tilt is introduced within A after its intersection with microtwin T. Furthermore, across A there is a visible displacement of the atomic columns. Fig. 3 is an HRTEM image obtained from a different part of the same epitaxial layer that shows the presence of defects A_1 and A_2 . Inserts (a) and (b) are images of defects A_1 and A_2 , respectively. Again notice a very slight misalignment of columns across the defect. Fig. 4(a) is an HRTEM image of the columnar defect A_2 from Fig. 3 with selected regions 1, 2, and 3 marked for diffractogram calculation. Fig. 4(b) shows DDFs of regions 1, 2 and 3. Note the spot splitting observed in the DDF from region 3.

The CDF image in Fig. 1 and the lattice images of Figs. 2 and 3 indicate the presence of defects lying on (110) planes of the GaP epilayer. DDFs in Fig. 4, obtained from the columnar defect marked as A_2 do not show satellite spots in a direction perpendicular to these boundaries. This indicates that structural integrity is maintained across the boundary, and this boundary is neither a grain boundary nor a twin boundary. In addition, Fig. 4(b) shows spot splitting (as indicated by arrows) for certain spots in the DDF obtained from region 3 in Fig. 4(a).

4. Discussion

Several significant observations emerge from the present study. First, CDF images show columnar $\{110\}$ type defects in epilayers after 500 s of growth. Second, HRTEM images indicate that in some cases these defects can extend from the epilayer/substrate interface to the surface. Third, careful examination of these defects by HRTEM

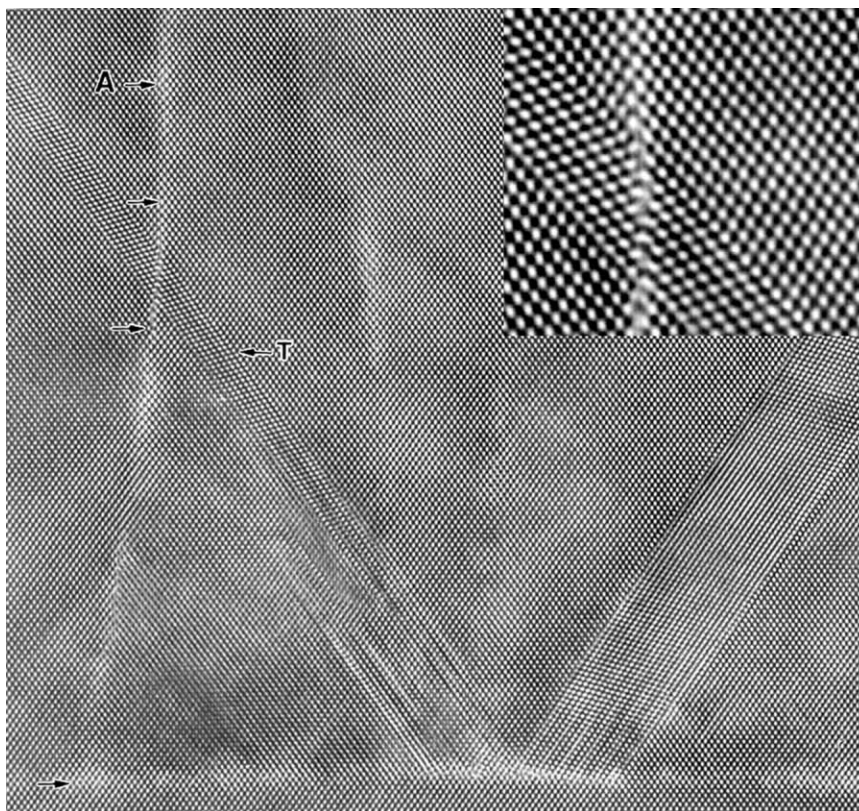


Fig. 2. $[1\bar{1}0]$ HRTEM image of a GaP epilayer on (001) Si after 500 s of growth at 420 °C that shows a columnar defect A intersecting a twin T. The insert is a magnified image of the columnar defect-twin intersection.

shows a slight displacement along the $[001]$ direction within the (110) plane. Fourth, twin intersection with these defects mostly results in the termination of the twin, though in some specific cases the twin can shear the defect.

In Fig. 1 the presence of contrast change across vertical boundaries parallel to the $\{110\}$ planes indicates that these are indeed $\{110\}$ type APB boundaries as first suggested by Holt [20] and then identified by Cohen and Carter [14], Kuan and Chang [16] and Ueda et al. [17]. In Fig. 5, we show in support of this assessment, a plot of the intensities of the transmitted beam, (002) and $(00\bar{2})$ (shown as $0\ 2$ and $0\ -2$, respectively) reflections from a $(1\bar{1}0)$ diffraction pattern of a perfect GaP crystal as a function of foil thickness (also known as a *Pendellosung* plot). As expected, the amplitudes of the two reflections for GaP are not equal for most thicknesses. Thus, in a (002) DF image,

the intensities from both sides of an APB should, according to Fig. 5, be different except at certain crystal thicknesses. The expected image contrast variation across an APB is observed for some of the vertical defects in Fig. 1.

Distinct boundary-like contrast, parallel to the (110) planes, is also observed in HRTEM cross-sectional images (Figs. 2 and 3). To verify that these are indeed APBs we have simulated the lattice image of a GaP crystal containing (110) type APBs. In our simulation, we have created an APB as detailed earlier in Section 2 and the resulting structure is schematically illustrated in Fig. 6. This translation is performed to change the occupation of the respective fcc sublattices across the boundary. Thus a Ga atom would be placed on a P position after the translation. The simulated HRTEM image for a through thickness focal series generated for the APB model is depicted in Fig. 7. The

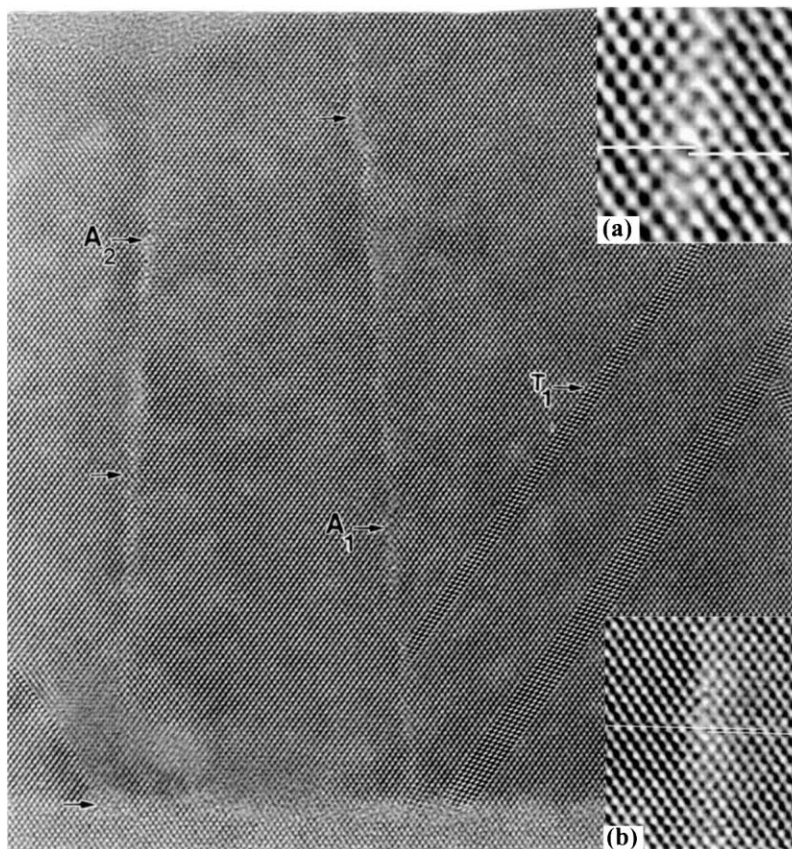


Fig. 3. $[1\bar{1}0]$ HRTEM image of GaP epilayer on (001) Si that indicate columnar defects A_1 and A_2 that are aligned parallel to $\{110\}$ planes. The inserts (a) and (b) are magnified images of A_1 and A_2 , respectively. Notice the slight displacement of black spots along the $[001]$ direction for both boundaries.

third row from the left indicates images near Scherzer defocus for different values of crystal thickness. These micrographs show that for a thin crystal <4 nm, the experimental lattice images do not show any evidence of the APB. However, for thicknesses in excess of 4 nm, Scherzer images do indicate a discernible displacement across the boundary along a $[001]$ direction, which gets accentuated with increasing thickness. Note that the black spots (which correspond to a doublet of Ga and P atoms) get shifted downwards when going from left to right. The experimental lattice images in Fig. 3 also reveal a slight displacement along the $[001]$ direction for the black spots, consistent with our simulated images.

Kuan and Chang [16] have reported that for a GaAs (110) APB, simulated lattice images do not

show the presence of an APB when imaged using a 200 kV TEM. To confirm their results, we have simulated a GaAs APB using our microscope parameters and the results are depicted in Fig. 8. Our images indicate that for various crystal thicknesses, the images do not show evidence of APBs, an assessment consistent with their results. However, Liliental-Weber et al. [11,21] have shown using a 1 MeV TEM, that APBs can be imaged in lattice images for GaAs indicating the sensitivity of APB identification to the operating voltage of the electron microscope.

The presence of APB contrast in lattice images of GaP and their absence in similar lattice images of GaAs for the same operating voltage may be related to the strain field associated with the formation of Ga–Ga, P–P and As–As bonds, which

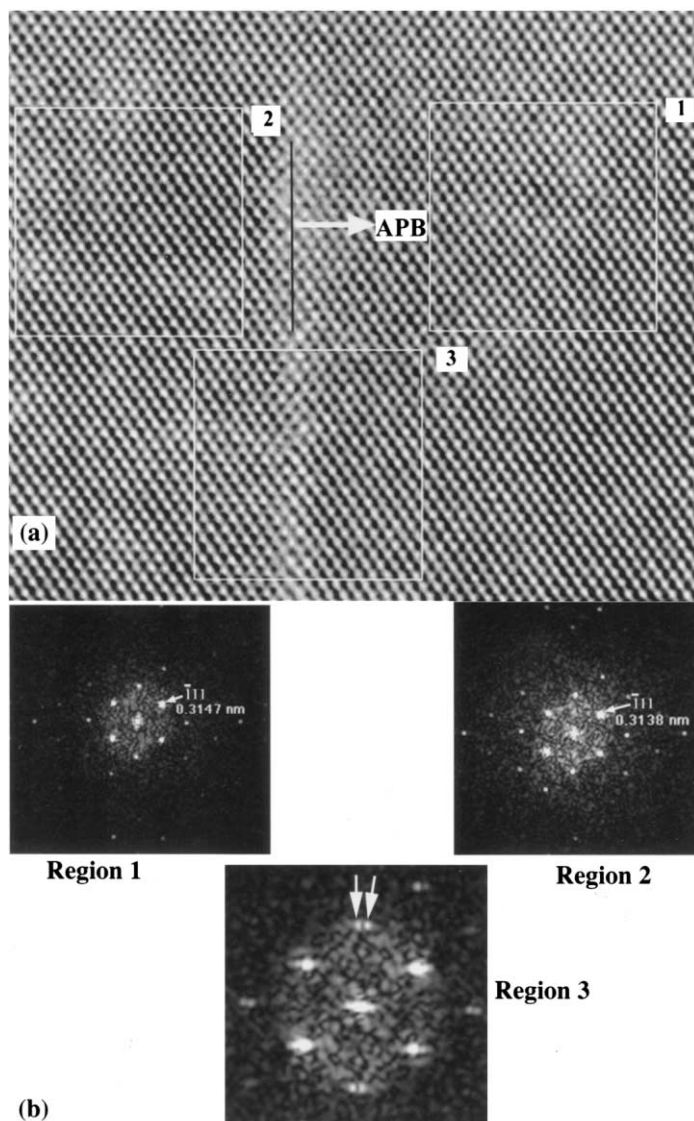


Fig. 4. (a) $[1\bar{1}0]$ HRTEM image of the columnar defect A_2 from Fig. 3 with selected regions marked for diffractogram calculation. (b) DDFs of regions 1, 2 and 3. Note the spot splitting observed in the DDF from region 3.

would result in a different planar spacing at the APB compared to the bulk crystal. Due to the formation of an APB, the sublattices will be translated with respect to each other and give rise to rigid body translations (\mathbf{R}). The tetrahedral covalent radii of Ga and As are 0.126 and 0.117 nm, respectively. Thus, it is conceivable that the associated \mathbf{R} is too small to be easily discernible in a lattice image. Rasmussen et al. [3,4] have shown

these rigid body displacements across an APB in GaAs can be calculated using the α fringe contrast method. They have obtained a value of $\mathbf{R} = 0.019$ nm along $[001]$, a fairly small value. Since the covalent tetrahedral radius of P (0.1 nm) atoms is smaller than that of As atoms, the value of \mathbf{R} is expected to be larger in GaP than that in GaAs.

Fig. 4 indicates splitting of the $\{002\}$ and $\{220\}$ type diffraction spots within the DDF obtained from

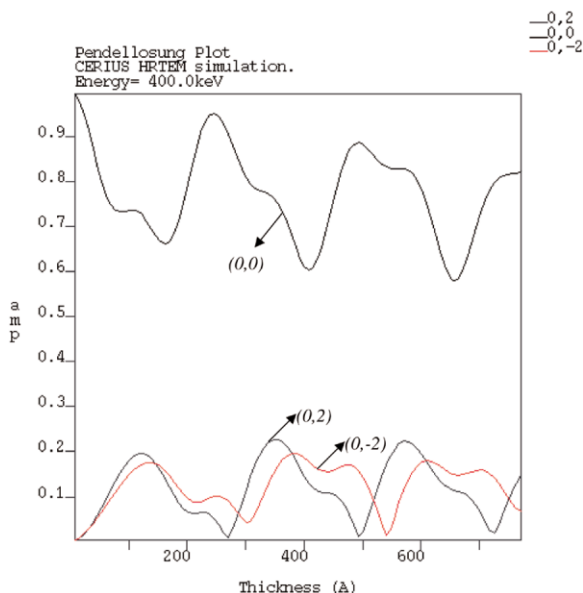


Fig. 5. A *Pendellosung* plot of a GaP crystal. Note the difference in diffracted intensity for the chemically sensitive (0,2) and (0,-2) reflections.

region 3. Van dyck et al. [22] have shown by optical simulations of high resolution images and by calculations based on kinematical theory that the presence of a single translation boundary can result in spot splitting such that the direction of splitting is normal to the boundary plane. The spots for which $\mathbf{H}\cdot\mathbf{R} \neq \text{integer}$ (\mathbf{H} : diffraction vector) are split and those for which $\mathbf{H}\cdot\mathbf{R} = \text{integer}$ are not split. Our results suggest therefore that since the $\{002\}$ and $\{220\}$ spots are split, a displacement \mathbf{R} is associated with this boundary that has components along the $[001]$ and $[110]$ directions. Simulations have shown that this kind of spot splitting is not discernible for $\{110\}$ GaAs APBs [23] indicating that the nature of the species at the APB affects the magnitude of the displacement vector.

The presence of APBs in III–V epitaxial layers grown on (001) Si have been associated with monoatomic surface steps on (001) Si (of height $a/4[001]$), where a is the lattice parameter [1,2]. If we assume that P forms a stronger bond with Si than Ga, then the first monolayer should be covered with P during GaP growth. Further growth on this P-terminated surface would lead to $\{110\}$ APBs. GaP islands grown on (001) Si will be

bounded by $\{111\}$ facets (the lowest energy facets, and an idealisation of the actual situation) such that two are terminated by Ga and two by P due to the non-centrosymmetry of the zinc-blende structure. The difference in surface energy of the $\{\bar{1}\bar{1}\bar{1}\}_P$ and $\{111\}_{Ga}$ facets would lead to the island taking on the shape of a truncated prism with one side elongated along one of the $\langle 110 \rangle$ directions of Si [24]. In addition, we have shown previously that these islands may be rotated by 90° to each other on the same terrace [24]. This observation suggests that surface reconstruction may not be playing a role in the nucleation of GaP islands on Si. Since in Si the two $\langle 110 \rangle$ directions are crystallographically identical, the probability of elongation in the mutually perpendicular $\langle 110 \rangle$ directions is equal. Thus, islands elongated along $[110]$ and $[1\bar{1}0]$ directions can be nucleated on the same terrace.

There are four possible situations for island coalescence and these are depicted in Fig. 9. On the same Si terrace, island facets terminated by the same species or by different species can coalesce as shown in Fig. 9(a,b). Coalescence can also occur across a monoatomic step and this situation is illustrated in Fig. 9(c,d). If the Si surface is uniformly covered by P atoms (i.e. the first atomic layer is P), then islands can coalesce on the same Si surface as shown in Fig. 10(a,b). The schematic suggests that even if we were to assume that wrong bonds are formed, these would not have well defined crystallographic features, and would be contrary to our experimental observations. The situation changes when islands coalesce across a surface step as shown in Fig. 10(c,d). An APB can form when a Ga-terminated facet coalesces either with another Ga-terminated facet across the step or a P-terminated facet across the step. In this case, by maintaining wrong bonds within the $\{110\}$ plane perpendicular to the interface plane, one can maintain APB free regions elsewhere. We can therefore infer that a $\{110\}$ type APB will not form by island coalescence on the same terrace.

There is also a possibility that the surface is not uniformly saturated with P (to balance the charge at the interface, local Ga–Si bonds in the first layer may be present) and thus there are areas on each terrace where the first atomic layer on Si is Ga-terminated. Coalescence of two islands which have

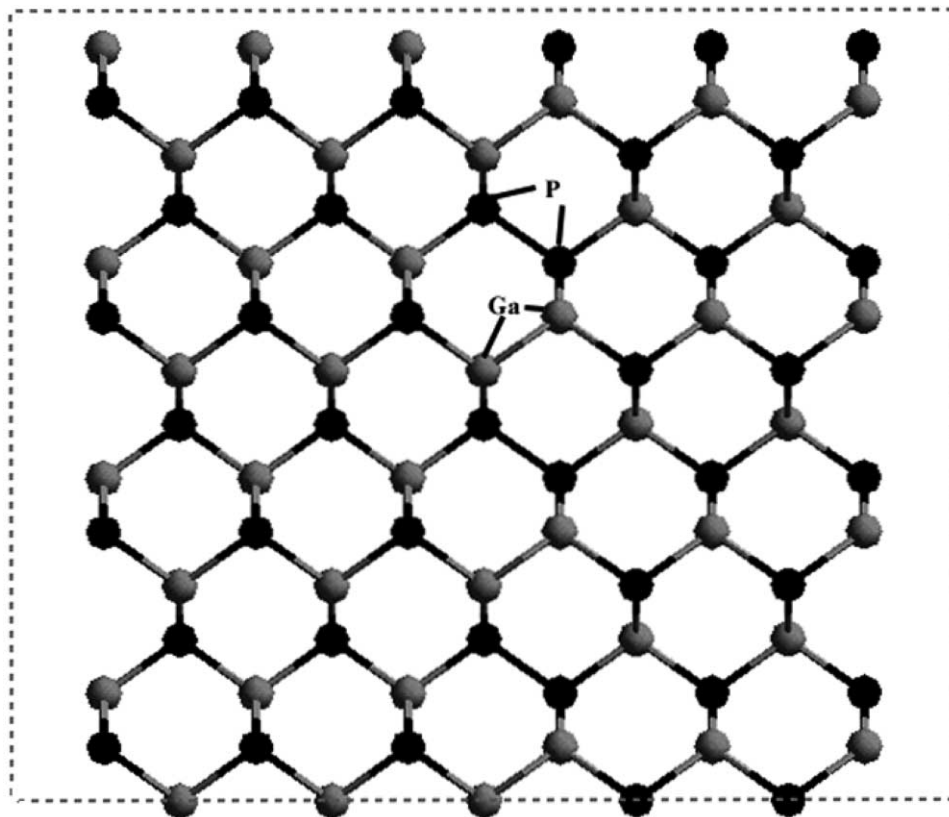


Fig. 6. The unit cell of a GaP crystal with a (110) APB that was used for simulation.

different species in the first atomic layer would give rise to {110} APBs in the same way as they would across a surface step on (001) Si. Our results have also shown that in some cases the boundaries extend all the way from the interface to the surface of the film and this is consistent with our idea that APBs will form at the point of coalescence. In some images, however, the boundary begins away from the interface and extends to the epilayer surface. This observation is not currently understood and could be a result of thickness variation across the film, such that they are no longer discernible below a certain thickness in lattice images as predicted by our simulations of Fig. 7.

In the analysis above, we have assumed that the islands are faceted on {111} planes. Our earlier results on island growth have shown that some islands may be faceted on the {110}, {112} and

{113} planes [24]. Coalescence of such islands would be more complicated, however, the analysis illustrates that independent of facet type, island coalescence in the absence of a surface step may not result in APB formation.

In Fig. 2 we see the intersection of an APB and a {111} microtwin, such that the APB gets tilted by $\sim 10^\circ$ as the twin propagates through. We have rationalized this observation assuming that the microtwin was formed after the formation of the APB. When viewed along a [110] direction, the twin would lie on the $(1\bar{1}1)$ plane. This twin could then have $\frac{a}{6}[\bar{1}12]$ Shockley bounding partials. If we consider only the APB displacement vector component that lies along a [001] direction, and if we consider the vector to be $\vec{A} = [001]$ and the

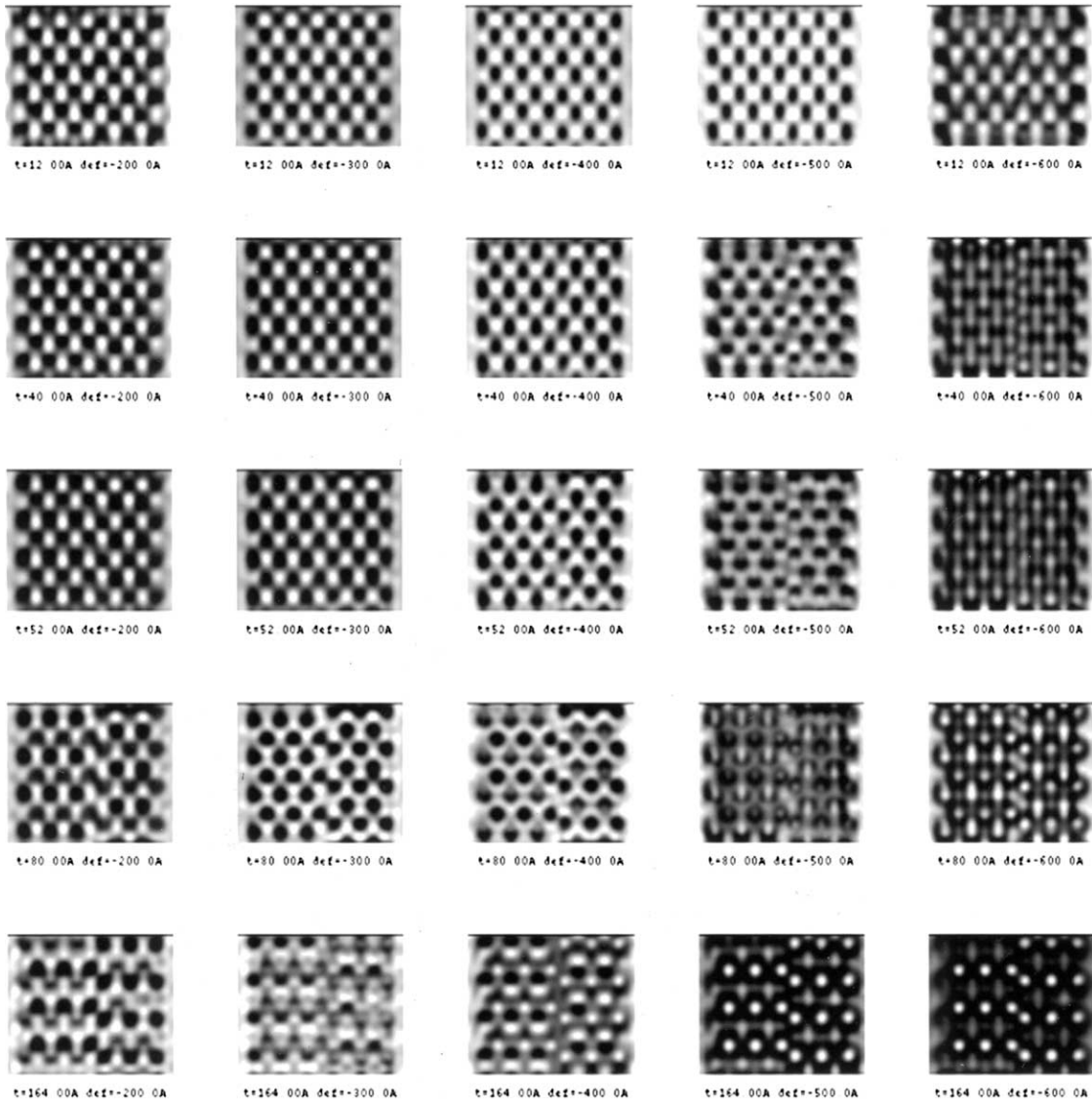


Fig. 7. A through thickness focal series obtained from the simulation of a {110} APB in GaP. The third row from the left corresponds to near Scherzer defocus.

Shockley partial $\vec{S} = \frac{a}{6}[\bar{1}12]$, then the resultant vector is given by, $\vec{B} = \vec{A} + \vec{S} = \frac{a}{6}[\bar{1}18]$. The angle between \vec{A} and \vec{B} is 10.08° . This value agrees well with the tilt produced in the APB direction when the twin propagates through it. We chose the

magnitude of \vec{A} to be the difference between the center of the two dark spots, also equal to the lattice parameter of GaP, since this is the smallest vector in the [001] direction within the lattice image that can be used to measure deviations. In some situations, a twin may stop at the APB plane. Such a situation is observed in Fig. 3 when T_1 ter-

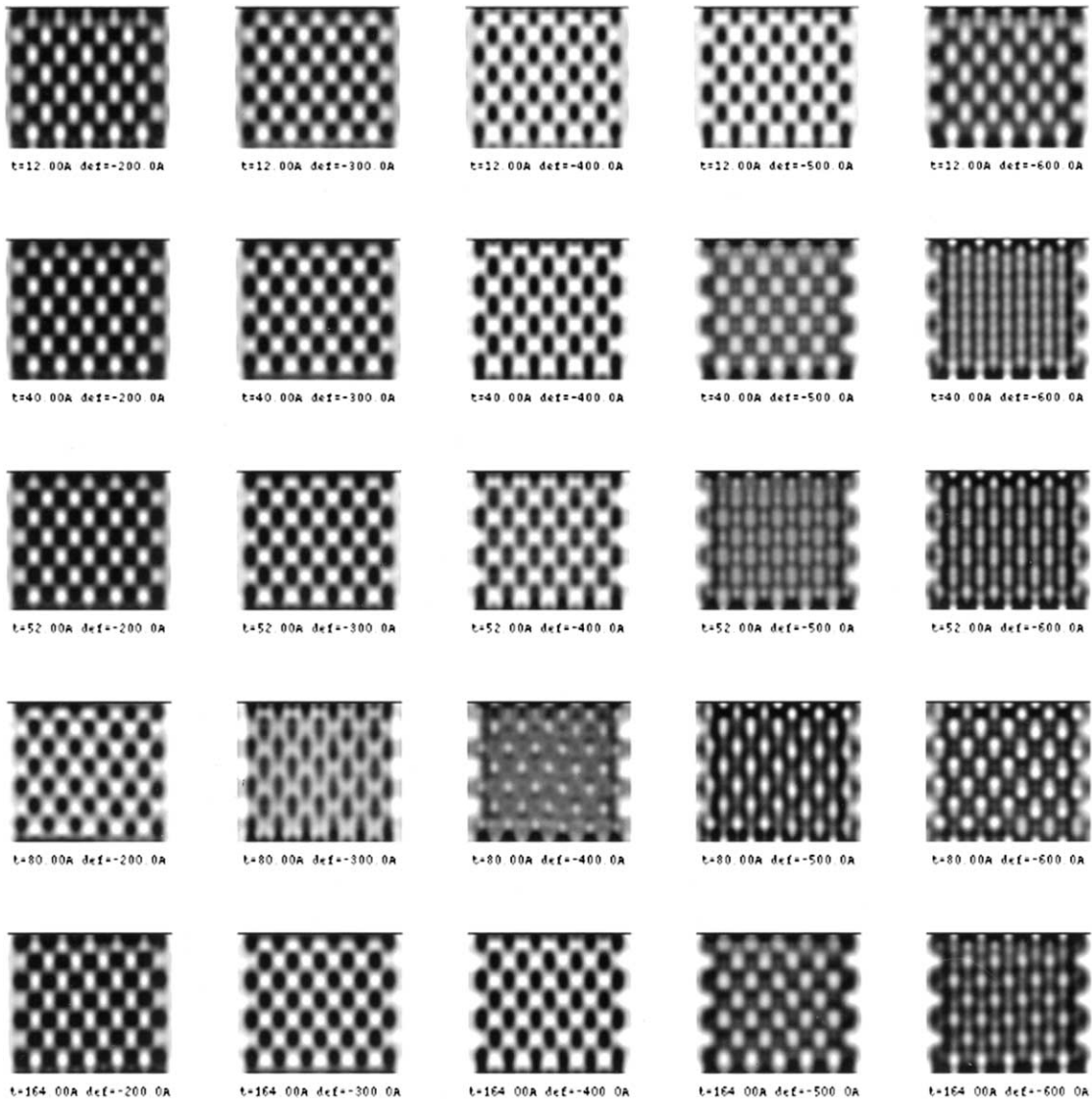


Fig. 8. A through thickness focal series obtained from the simulation of a $\{110\}$ APB in GaAs. The third row from the left corresponds to near Scherzer defocus.

minates on A_1 . This situation may occur when there are kinetic barriers to the twin propagation through an APB and is a phenomenon which has been observed previously in GaAs/Si (001) [11].

Our results have shown that most of the APBs lie along $\{110\}$ planes that in some cases extend all the way from the interface to the surface of the film. To our knowledge this is the first study of APB evolution within thin epilayers of III–V/Si

(<100 nm) by TEM. Work on thicker films of GaAs/Si (001) have revealed through cross-sectional TEM that APBs tend to get eliminated by closing on themselves [8,11,25]. This can happen when $\{110\}$ oriented APBs bend to other crystallographic directions such as $\{111\}$ and $\{113\}$ and then back to $\{110\}$. This is explained as an effect of antiphase domains being energetically unfavourable since APBs have inherently high energy. With

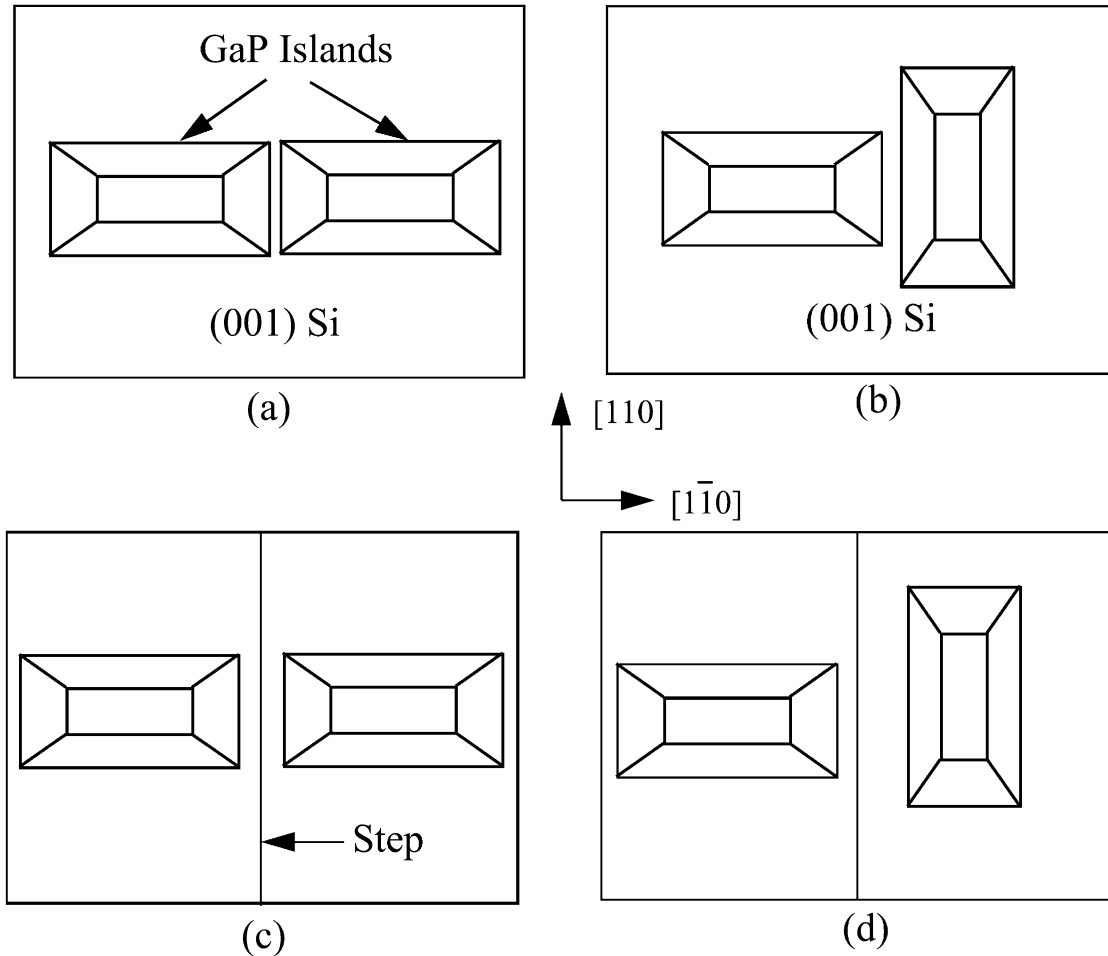


Fig. 9. (a,b) depict situations when islands are on the same Si terrace. (c,d) depict situations when islands are on two contiguous terraces separated by a monatomic step on a Si (001) surface.

increasing thickness, the increase in energy due to these large antiphase domains, provides the necessary impetus for a $\{110\}$ APB to bend to the high energy $\{111\}$ or $\{113\}$ APB configurations, i.e. energetically it is favourable to bend the APB to high energy configurations so as to close on itself rather than remain a $\{110\}$ type APB through the thickness of the film. As a result of this bending, the APBs get annihilated at thicker layers $>3 \mu\text{m}$.

Lambrecht et al. [26] have shown using density functional theory that APB energy depends not only on wrong bonds per unit area as suggested by Petroff [27], but also on their degree of mutual compensation and charge state (related to doping

or interaction with other defects). Their theory predicts that locally compensated APBs (in their terminology, APBs with an equal number of wrong bonds of opposite type as near neighbors in the same interface, for e.g., $\{110\}$ APBs) should dominate in stoichiometric GaAs. They also suggest that the doping of the layers may in some cases stabilize $\{111\}$ and $\{001\}$ APBs (n-type doping may favor Ga–Ga $\{001\}$ APBs) which have incompletely compensated bonds and allow the possibility of APB annihilation. The stability issue of APB facet planes remains unclear. However, contrary to the APB annihilation observations in thick epilayers $>100 \text{ nm}$, we observe very little

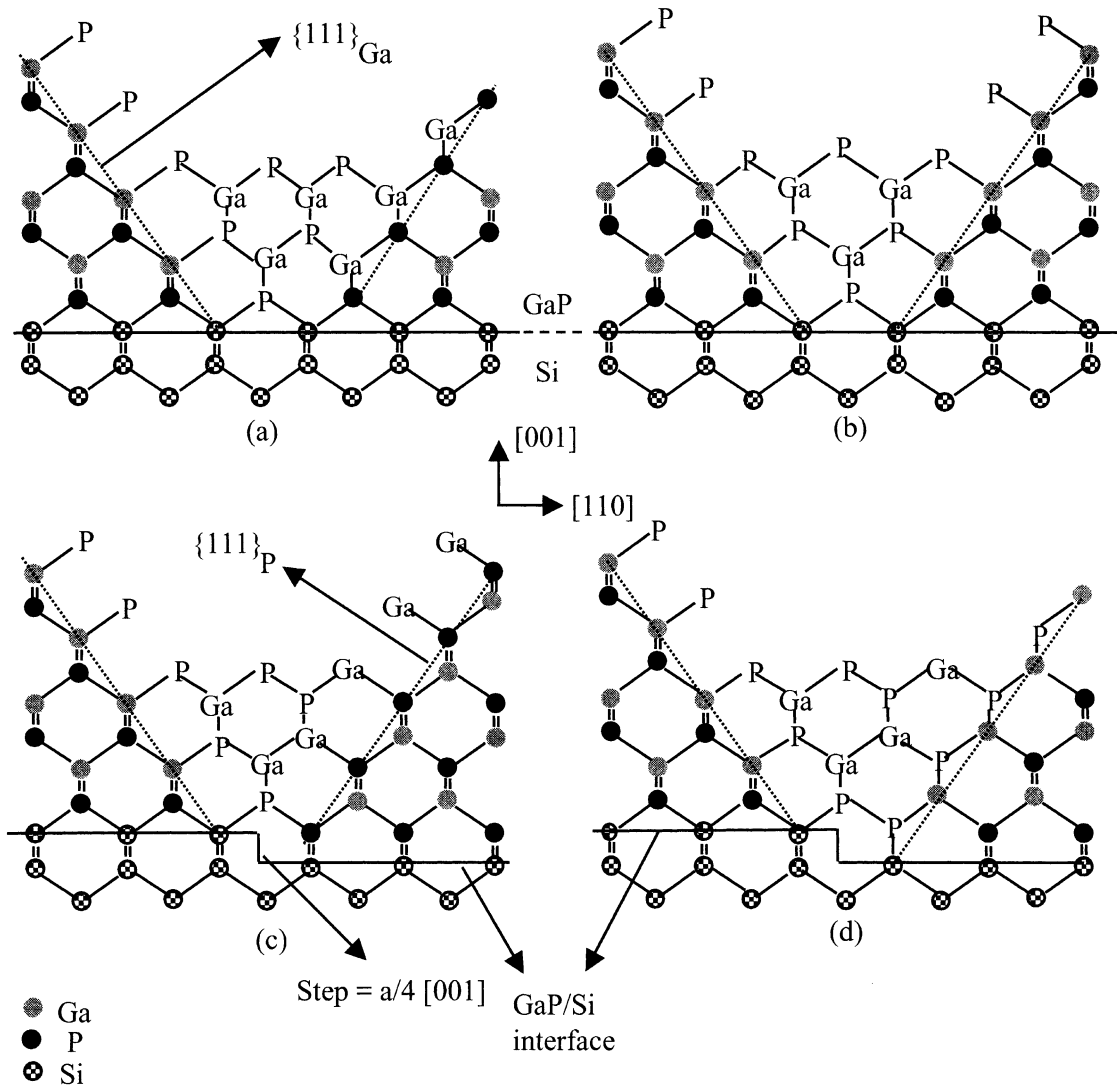


Fig. 10. (a,b) Coalescence of {111} faceted islands on the same Si terrace. (c,d) Coalescence of {111} faceted islands across a monatomic step on (001) Si.

bending of APBs and this is attributed to the smaller thickness of the epilayers which may not allow the APBs to achieve their low energy configurations.

5. Conclusions

1. Planar, columnar features lying on {110} planes within GaP epitaxial films grown on (001) Si

have been shown to exist at the early stages of GaP island coalescence by HRTEM and CDF-TEM. The planar boundary observed by HRTEM was compared with simulated images to confirm that they are APBs. The presence of spot splitting within DDFs obtained from the boundary is indicative of a translation interface with a displacement vector R from Ga–Ga and P–P wrong bonds at the interface.

2. The origin of {110} APBs is attributed to island

coalescence across monatomic steps. It has been shown that island coalescence on the same terrace in the absence of a surface step may not lead to {110} APBs. However, islands that coalesce across a step can form APBs independent of the nature of the terminating island facets.

Acknowledgements

VN and SM would like to acknowledge the Center for High Resolution Electron Microscopy (CHREM) at Arizona State University for use of TEM and computing facilities. VN would also like to thank Prof. Marc DeGraef at Carnegie Mellon University for useful discussions on APB identification and for pointing out the relevant reference for spot splitting. All the authors would like to gratefully acknowledge the support of this work by DOD-MURI grant F49620-95-1-0447.

References

- [1] Kroemer H. *J Cryst Growth* 1987;81:193.
- [2] Kroemer H. *J Vac Sci Technol B* 1987;5:1150.
- [3] Rasmussen DR, Mckernan S, Carter CB. *Phil Mag A* 1991;63:1299.
- [4] Rasmussen DR, Mckernan S, Carter CB. *Phys Rev Lett* 1991;66:2629.
- [5] Kroemer H, Polasko KJ, Wright SL. *Appl Phys Lett* 1980;36:763.
- [6] Aspnes DE, Ihm J. In: Fan JCC, Phillips JM, Tsaur BY, editors. *Heteroepitaxy on silicon II*. Pittsburgh: Materials Research Society; 1987:45.
- [7] Uppal PN, Kroemer H. *J Appl Phys* 1985;58:2195.
- [8] Georgakilas A, Stoemenos J, Tsagaraki K, Komninou P, Flevaris N, Panyotatos P, Christou A. *J Mater Res* 1993;8:1908.
- [9] Pukite PR, Cohen PI. In: Fan JCC, Phillips JM, Tsaur BY, editors. *Heteroepitaxy on silicon II*. Pittsburgh: Materials Research Society; 1987:51.
- [10] Tafto J, Spence JCH. *J Appl Cryst* 1982;15:60.
- [11] Liliental-Weber Z, Weber ER, Parechianian-Allen L, Washburn J. *Ultramicroscopy* 1988;26:59.
- [12] Posthill JB, Tam JCL, Das K, Humphreys TP, Parikh NR. *Appl Phys Lett* 1988;53:1207.
- [13] Gowers JP. *Appl Phys A* 1984;34:231.
- [14] Cohen D, Carter CB. In: Michel J, Kennedy T, Wada K, Thonke K, editors. *Defects in electronic materials II*. Pittsburgh: Materials Research Society; 1997:503.
- [15] Holt DB. *J Phys Chem Solids* 1969;30:1297.
- [16] Kuan TS, Chang CA. *J Appl Phys* 1983;54:4408.
- [17] Ueda O, Soga T, Jimbo T, Umeno M. *Appl Phys Lett* 1989;55:445.
- [18] Narayanan V, Mahajan S, Bachmann KJ, Woods V, Dietz N. 2001, in press.
- [19] Cerius, version 3.2. Cambridge (UK): Molecular Simulations Inc, 1993.
- [20] Holt DB. *J Mater Sci* 1984;19:439.
- [21] Liliental-Weber Z, O'Keefe M, Washburn J. *Ultramicroscopy* 1989;30:20.
- [22] Van Dyck D, Van Tendeloo G, Amelinckx S. *Ultramicroscopy* 1984;15:357.
- [23] Degraef M. private communication, 1999.
- [24] Narayanan V, Mahajan S, Sukidi N, Bachmann KJ, Woods V, Dietz N. *Phil Mag A* 2000;80:555.
- [25] Molina SI, Aragon G, Garcia R. *J Electron Mater* 1993;22:567.
- [26] Lambrecht WRL, Amador C, Segall B. *Phys Rev Lett* 1992;68:1363.
- [27] Petroff PM. *J Vac Sci Technol B* 1986;4:874.